Journal of Mechanics Engineering and Automation 2 (2012) 41-51

Clearance Effects in Parallel Manipulators: Position Error Discontinuities and Inertial Effects Influence

Oscar Altuzarra[1], Jokin Aginaga[2], Charles Pinto[1] and Xabier Iriarte[2]

1. Department of Mechanical Engineering, Faculty of Engineering, Univ. of the Basque Country, UPV/EHU, Bilbao 48013, Spain

2. Mechanical, Energetics and Materials Engineering Department, Public University of Navarre, Pamplona 31006, Spain

Received: September 15, 2011 / Accepted: October 11, 2011 / Published: January 25, 2012.

Abstract: Clearances at joints cause an uncertainty in the actual posture of the end-effector of any mechanism. This uncertainty relays on the clearance dimension and the way these clearances are taken up by the mechanism under the load and the inertial effects at every instant. As a matter of fact, the actual measure of the pose error is often replaced by an uncertainty measure. However, a side effect of the existence of clearances is that they can cause sudden changes in the posture of the mechanism as a motion is performed. Such discontinuities in the position produce task defects and impacts. In this work a tool to determine the pose error due to clearances is presented together with a discontinuity analysis. In addition, effects of mass distribution and inertial effects on such discontinuities are expounded, taking a 3-PRS robot as example.

Key words: Parallel manipulator, clearance, position error, discontinuity.

1. Introduction

Parallel manipulators have a loss of accuracy because of manufacturing and assembly errors. When ideal joints are considered these errors can be corrected with an appropriate calibration. However, clearance in joints is unavoidable and it is often necessary to a certain extent to provide a smooth motion. This leads to position uncertainty and instability when inputs are locked.

Several authors have analyzed clearance influence on position error using different ways of analysis. Some of them evaluate the maximum position error or most probable final positions of the end-effector, by means of geometrical or kinematical methods. The former use the position problem or rely solely in the geometric characteristics derived of a simple modelling of the clearances [1-2]. The latter consider that the slop of the mechanism due to clearances is so small that it can be evaluated approximately with a velocity analysis [3-5]. Other authors carry out a deterministic approach trying to get the actual error in the end-effector pose under the actions of the load on the manipulator. The deterministic approach can be executed by means of kinetostatic or dynamic analysis. The first step is to get actual reactions on the joints of the mechanism. With them, by calculating the relative position between the pin and the hub of joints with clearance, the error contribution at each joint is added to the end-effector pose error [6-8]. In the dynamic analysis, the calculated joint reactions are introduced as external generalised forces into the dynamic model. Also, contact forces inside imperfect joints are described with more detail taking into account the three kind of relative motion (free-flight, impact and continuous contact) [9-11].

In this work, a numerical analysis of the error pose of the end-effector is presented where the authors have tried to keep the simplicity of the procedures based in kinematical methods that consider rigid bodies, while

Corresponding author: Jokin Aginaga, Ph.D., research fields: kinematics, dynamics and accuracy analysis of parallel manipulators. E-mail: jokin.aginaga@unavarra.es.

adding external and inertial loads. Applied to a 3-PRS manipulator, where P stands for a prismatic actuated joint, R for a revolute joint and S for a spherical one, this analysis provides locations where discontinuities occur due to sudden changes in contact modes. Effects of each kind of clearance on such discontinuities are also analyzed. Finally, the influence of mass distribution of the mobile platform on the location of the discontinuity steps is studied.

The paper is organized as follows: Section 2 describes the error calculation procedure. In section 3, the described procedure is applied to the workspace of a 3-PRS manipulator. Also, a kinetostatic discontinuity analysis is presented, determining the influence of each clearance on discontinuities and showing how mass distribution changes the error distribution. Section 4 includes dynamic effects, comparing kinetostatics and dynamics results along a trajectory. Finally, some concluding remarks are presented in section 5.

2. Clearance Error Analysis

The first tool that we need to develop is a powerful procedure for the analysis of pose errors due to clearances. This procedure includes the possibility of applying any external or inertial load to any link of the mechanism. It evaluates reactions at joints to decide the way clearances are actually taken up. Then, it finds the end-effector pose error with a kinematic approximation, considering joint clearances, and allowing for pose corrections in passive joints.

The procedure includes the following modules:

Modelling of clearances:

- Inverse Kinematics of the Nominal Mechanism, i.e., position, velocities and accelerations. It will analyze the ideal mechanism to solve the nominal kinematics over a desired path or the workspace;
- Statics or Dynamics of the Nominal Mechanism. By means of a Newton-Euler analysis, the wrenches at the joints under the external and/or inertial loads of the nominal mechanism will be calculated;
- Accuracy analysis: Our approach is to employ a deterministic method using the kinematic velocity relations. For every posture, we will use the joint reactions to define the infinitesimal displacements due to clearances at every joint. With fixed inputs and the velocity equations at the posture analyzed, we will obtain changes in the passive joint variables due to clearances, and then the end-effector pose error;
- Numerical analysis of discontinuities: The pose error will show if clearance take-up changes suddenly at some postures, and which clearance causes this. These sudden changes appear at certain poses depending on the configuration of the mechanism and the applied wrenches. Said poses determine a so-called discontinuity locus.

A schematic view of the pose error calculation procedure is described in Fig. 1, where terms surrounded by an ellipse represent data and rectangles are the different modules of the procedure. These all are thoroughly described in what follows.

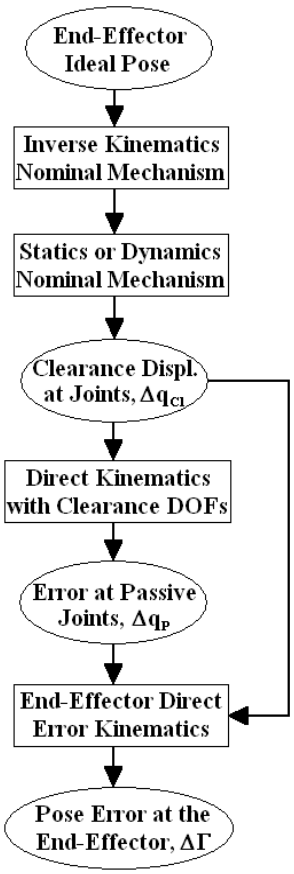

Fig. 1 Schematic view of the error calculation procedure.

2.1 Modelling Clearances

Before starting with the analysis of pose errors, it is necessary to define how clearances are taken up. By way of example, we will use in the sequel a tripod parallel manipulator shown in Fig. 2.

This is a three degrees of freedom (DOF) mechanism defined by three limbs of the type PRS. The three DOFs of the mobile platform are angles Ψ and Θ about *x* and *y* axes respectively, and the coordinate Z. However, coordinates X and Y and angle Φ about z axis do not remain immobile; they have parasitic motions due to the architecture of the manipulator as described in Ref. [12]. It is supposed that both passive pairs (R and S) have clearance.

Fig. 3 shows a 3-PRS prototype built at the University of the Basque Country. Its prismatic actuators lie on a circle with a radius of 0.18 m. Links BiAi are 1 m long and the radius of the mobile platform (distance PAi) is 0.36 m. The mass of the mobile platform is 9.8 kg and that of the BiAi links is 3 kg.

Regarding the revolute pair clearance, we will use local reference frames at each limb ($\mathbf{x_j}$, $\mathbf{y_j}$, $\mathbf{z_j}$) where $\mathbf{x_j}$ is in radial direction, $\mathbf{y_j}$ follows the direction of the revolute pair, and $\mathbf{z_j}$ is vertical (Fig. 2). First, axial displacements due to clearance are Δy_{Bj}, and radial one to be decomposed into horizontal and vertical directions Δx_{Bj} and Δz_{Bj}. Second, an angular motion caused by the reaction couple will be used, $\Delta\theta_{Bj}$ in the direction of the couple.

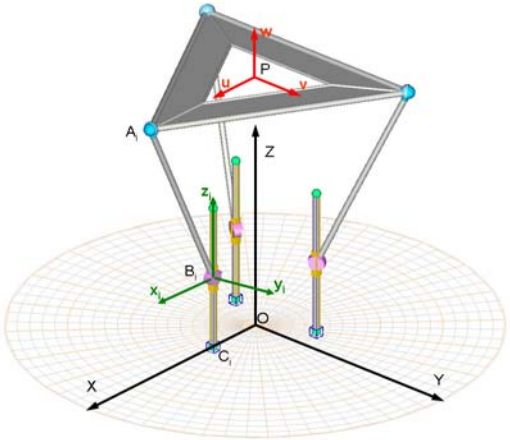

Fig. 2 3-PRS parallel manipulator.

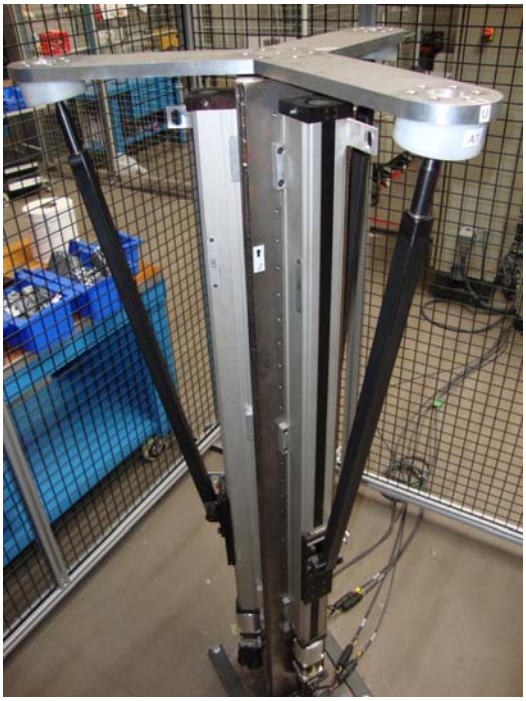

Fig. 3 3-PRS parallel manipulator prototype.

For simplicity, axial, radial and angular clearances are separated and treated independently. A revolute joint with clearance is shown in Fig. 4, where axial clearance is denoted as *a* and radial clearance as *r*.

In the spherical pair, radial clearance is considered and then displacements in the three directions of the space are considered, namely Δx_{Aj}, Δy_{Aj} and Δz_{Aj} . Fig. 5 shows a spherical joint with clearance, where *s* represents the magnitude of the radial clearance.

2.2 Inverse Kinematics of the Nominal Mechanism

The first module solves the inverse position problem in the nominal mechanism shown in Fig. 2. Actuated P joints are at B_j in the direction of $\mathbf{z_j}$, passive R joints are at B_j in the direction of $\mathbf{y_j}$, spherical joints are at points A_j of the mobile platform, and the tool-centre-point (TCP) is at *P*. A fixed frame (**i**, **j**, **k**) is placed at *O*, and a moving frame (**u**, **v**, **w**) is attached at reference point *P* on the mobile platform.

Each limb constraints the motion of the vertex A_j to the corresponding vertical plane Πj that contains points *O*, B_j and C_j, and has a characteristic vector $\mathbf{u_j}$, which corresponds to $\mathbf{y_j}$. Therefore, the posture variables of the mobile platform must fulfill three constraint equations.

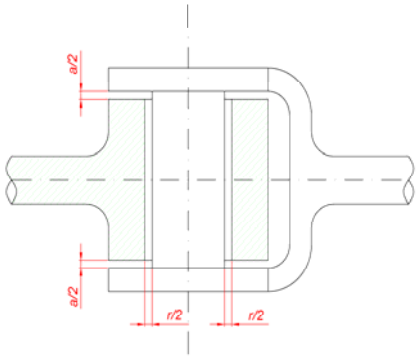

Fig. 4 Clearance at R joints.

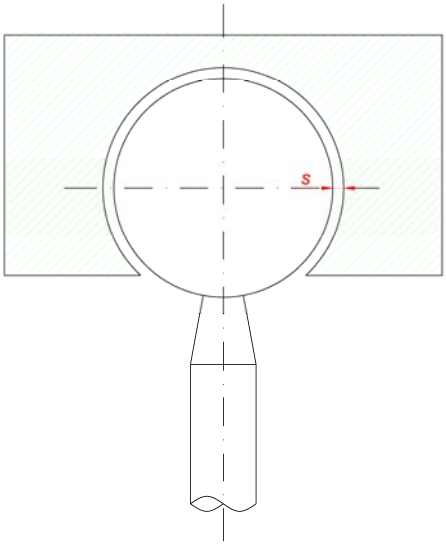

Fig. 5 Clearance at S joints.

Denoting the position vector of the TCP as **p** and position vector of the vertices of mobile platform as $\mathbf{a_j}$, constraint equations result as follows:

$$\mathbf{a_j} \bullet \mathbf{u_j} = 0; \quad j = 1,\ldots,3 \tag{1}$$

where

$$\mathbf{a_j} = \mathbf{p} + (\mathbf{a_j} - \mathbf{p}); \; j = 1,\ldots,3 \tag{2}$$

The output variables that define the posture of the mobile platform are the coordinates of the TCP, i.e., [X, Y, Z]^T, and the three angles used for the orientation of the mobile platform with respect to the fixed frame. The latter will be taken as the angles of orientation about the fixed reference axes: firstly an angle Φ about the *z* axis, secondly an angle Ψ about the *x* axis, and finally an angle Θ about the *y* axis [12].

In order to solve inverse kinematics, variables Z, Ψ and Θ are used as independents whereas X, Y and Φ are the aforementioned parasitic motions. These are defined by means of constraint equations, which, for a mobile platform that is an equilateral triangle where PA_i is r_p, result in:

$$\Phi = \tan^{-1}\left(\frac{s\Psi\, s\Theta}{s\Psi + s\Theta}\right) \tag{3}$$

$$Y = -r_p c\Psi s\Phi \tag{4}$$

$$X = \frac{r_p}{2}\left(c\Theta c\Phi - c\Phi c\Psi + s\Psi s\Theta s\Phi\right) + \frac{r_p}{2}\sqrt{3}\left(c\Theta s\Phi - s\Psi s\Theta c\Phi + c\Phi c\Psi\right) \tag{5}$$

where *c* and *s* stand for cosine and sine respectively.

Once the posture of the mobile platform is completely determined by the constraint equations in Eq. (3), it is feasible to state the resolution of each limb apart. By imposing that $(\mathbf{a_j} - \mathbf{b_j})$ is constant at all times, we can state the following system of non-linear equations:

$$|\mathbf{a_j} - \mathbf{b_j}| = L_j, \;\; j = 1,\ldots,3 \tag{6}$$

where $\mathbf{b_j}$ is the position vector of the revolute joint *j* and L_j is the length of the links B_iA_i.

For the velocity analysis of the tripod, first we must differentiate the constraint equations and then the loop closure equations. Both will be added together to produce the Jacobian equations. And further differentiation will be used to obtain the accelerations.

2.3 Statics or Dynamics of the Nominal Mechanism

Merlet [13] mentions flight simulators, pick-and-place, vibration simulation and even high-speed machining tools as applications where dynamics play an important role. On the other hand, there are applications where high accelerations are not required and then inertial effects can be neglected, such as machine tools, micro-positioning and surgical robots. Taking this fact into account, this work analyses separately kinetostatics and dynamics. Anyway, since statics are a particular case of dynamics, equations are presented with inertial loads.

For every instant considered and once the inverse problems are solved, an inverse dynamics problem can be used to obtain the forces $\mathbf{f_{Ji}}$ and moments $\mathbf{m_{Ji}}$

exerted by one link on its neighbours at the joint *i*. Using a Newton-Euler approach, it is possible to obtain a linear system of equations where external loads, gravity forces, and inertial loads are known and appropriately accounted for. For each link *k* we get:

$$\mathbf{f_{Ji}} + \mathbf{f_{ek}} + [-m_k \mathbf{a_k}] = \mathbf{0} \quad (5)$$

$$\mathbf{m_{Ji}} + \mathbf{r_{Ji}} \times \mathbf{f_{Ji}} + \mathbf{m_{ek}} + \mathbf{r_{Ek}} \times \mathbf{f_{ek}} + [-\mathbf{I_k}\,\omega_k - \dot{\omega}_k \times \mathbf{I_k}\,\omega_k - \mathbf{r_{Ck}} \times m_k\,\mathbf{a_k}] = \mathbf{0} \quad (6)$$

where $\mathbf{f_{ek}}$ and $\mathbf{m_{ek}}$ form the wrench of external load, $\mathbf{r_{Ek}}$ is the position vector of the point E_k where such forces are applied, m_k is the mass of the link *k*, and $\mathbf{a_k}$ is the acceleration of the centre of mass of the link *k*.

Once all links have been considered, all equations are assembled and included in the next system of equations:

$$\mathbf{A} \cdot \mathbf{w_J} = \mathbf{w_e} + \mathbf{w_I} \quad (7)$$

where $\mathbf{w_J}$ is the unknown vector of joint reactions, $\mathbf{w_e}$ and $\mathbf{w_I}$ represent the known external wrenches and inertial wrenches, and $\mathbf{A}$ is a matrix built from the equilibrium equations and that depends on the posture.

Solving Eq. (7), joint reactions $\mathbf{f_{Ji}}$ and moments $\mathbf{m_{Ji}}$ at every joint J_i are obtained. From these results we obtain the contact mode at the joint and assign the way clearances are taken up. These infinitesimal variations in clearance joints are grouped in vector $\mathbf{\Delta q_{Cl}}$.

2.4 Direct Error Kinematics with Clearance DOFs

Using screw coordinates allows a compact matrix formulation of the velocity equations. Let *P* be the reference point of the end-effector, then end-effector twist is defined by

$$\$_P = \begin{bmatrix} \omega \\ \dot{p} \end{bmatrix} \quad (8)$$

and it can be calculated for the nominal mechanism by summing contributions from each joint *i* at a limb *j*, going from the fixed frame to the end-effector:

$$\$_P = \sum_{i=1}^{N_j} \dot{q}_i^{\,j} \hat{\$}_{J_i}^{\,j} \quad (9)$$

where N_j is the number of joints of the limb *j*, and $\dot{q}_i^{\,j}$ and $\hat{\$}_{J_i}^{\,j}$ are, respectively, the rate and the screw at each joint *i* of said limb.

For a fully parallel manipulator with *n* limbs, the number of independent loops will be equal to (*n*–1). As $\mathbf{\$_P}$ can be calculated using each kinematic chain, for every closed loop of a mechanism it can be written:

$$\sum_{i=1}^{N_{j+1}} \dot{q}_i^{\,j+1} \hat{\$}_{J_i}^{\,j+1} - \sum_{i=1}^{N_j} \dot{q}_i^{\,j} \hat{\$}_{J_i}^{\,j} = 0 \quad (10)$$

where $j = 1, \ldots, (n-1)$.

Terms of Eq. (10) can be separated into those of the passive joints and those of actuated joints. Assembling equations of each closed loop, denoting the passive joints with index P and the actuated or input joints with I, and reordering the terms, an equation system can be built in order to solve the nominal velocity analysis:

$$\mathbf{J_P} \cdot \dot{q}_P = \mathbf{J_I} \cdot \dot{q}_I \quad (11)$$

where matrix $\mathbf{J_P}$ is a square matrix for fully parallel manipulators.

Additional freedoms due to clearances can be added to the mechanism and then to Eq. (11), yielding:

$$\mathbf{J_P} \cdot \dot{q}_P = [\mathbf{J_I}\,\mathbf{J_{Cl}}] \cdot \begin{bmatrix} \dot{q}_I \\ \dot{q}_{Cl} \end{bmatrix} \quad (12)$$

where $\mathbf{J_{Cl}}$ is a matrix with the screws from freedoms due to clearances and $\dot{q}_{Cl}$ are their velocities.

Assuming that displacements are infinitesimal, they can be approximated by velocities. If the actuated joints are fixed, i.e., $\mathbf{\Delta q_I} = \mathbf{0}$, and relative positions between the two parts of each joint $\mathbf{\Delta q_{Cl}}$ are determined using the reactions calculated in the joint wrenches analysis, then the motion at passive joint freedoms $\mathbf{\Delta q_P}$ due to clearance take up can be obtained from

$$\mathbf{J_P} \cdot \mathbf{\Delta q_P} = \mathbf{J_{Cl}} \cdot \mathbf{\Delta q_{Cl}} \quad (13)$$

2.5 End-Effector Direct Error Kinematics

Once clearance displacements at joints ($\mathbf{\Delta q_{Cl}}$) and the motions at passive freedoms they produce ($\mathbf{\Delta q_P}$) are obtained, the error pose of the end-effector can be calculated with Eq. (9) as follows:

$$\mathbf{\Delta\Gamma} = \begin{bmatrix} \Delta\alpha \\ \Delta p \end{bmatrix} = \begin{bmatrix} \hat{\$}_J^{\,j} & \hat{\$}_{Cl}^{\,j} \end{bmatrix} \begin{bmatrix} \Delta q_J^{\,j} \\ \Delta q_{Cl}^{\,j} \end{bmatrix} \quad (14)$$

where Δp is the error in position of point *P* due to clearance take up, and $\Delta\alpha$ is the change in the

absolute orientation of the end-effector due to clearances. Superindex*j* means that $\Delta\Gamma$ can be calculated using any limb *j* of the manipulator.

Vector $\Delta\Gamma$ is the pose error of the end-effector, i.e., by adding $\Delta\Gamma$ to the nominal pose of a mechanism, the actual pose is obtained.

Near direct singularities, the poor conditioning of matrix **A** of Eq. (7) leads to the methodology of error calculation performing inadequately, since infinitesimal displacements can not be approximated by velocities.

3. Kinetostatic Discontinuity Analysis

In Ref. [6], authors showed that sudden changes in ideal link load lead to discontinuities in a four-bar linkage trajectory. Likewise, a way to find out the location of discontinuities is presented in Ref. [8]. Other authors describe different contact modes between the two parts of a joint. In Ref. [14], the switch from tension to compression in the legs of the Generalised Stewart Platform leads to discontinuities in position and orientation error. In a similar way, changes in the contact modes have been shown to produce discontinuities in the position error in a 3-UPU robot in Ref. [7], where U stands for a Universal joint and P for a prismatic actuated joint.

In our work, these staircase-shaped values or sudden changes in contact modes are represented as discontinuities in the position. A discontinuity represents a neighbourhood of the workspace where error due to clearances can undergo a step-like change. At those poses it is not easy to define the relative position between the two parts of a joint, leading to an error uncertainty.

Using a kinetostatic analysis, i.e., no inertial terms in Eq. (5), position error can be calculated in a workspace with fixed Z. In Fig. 6, color represents the magnitude of error due to clearances in the 3-PRS for any value of Ψ and Θ, for the mechanism loaded only with the dead weight of its components. Pose error at the mobile platform is represented by position error at its Centre of

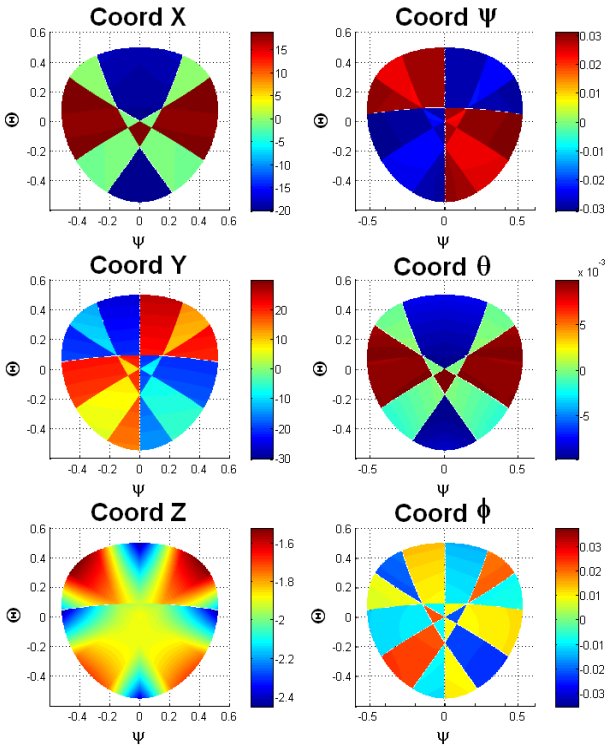

Fig. 6 Error maps due to clearances using a kinetostatic analysis in the workspace.

Gravity and infinitesimal variations in the orientation of the end-effector. In turn, sudden changes in colour identify discontinuities. It can be noticed that the workspace can be divided in areas free of discontinuities.

In order to know which clearance produces the discontinuity they can be analysed one by one, since they have been considered independent to each other. Figs. 7-10 represent the influence of each clearance of the joints on the position error.

Figs. 7-8 do not show discontinuities in the Ψ-Θ workspace. Then, clearance at spherical joints and radial clearance at revolute joints do not produce sudden changes in the position error. Accordingly, these clearances are not critical for such a workspace with the current load distribution. On the other hand, Figs. 9-10 illustrate several sudden changes on the graphics colour, i.e., several error discontinuities. Consequently, axial and angular clearances of the revolute joint can produce the undesired discontinuities on the actual position of the mobile platform.

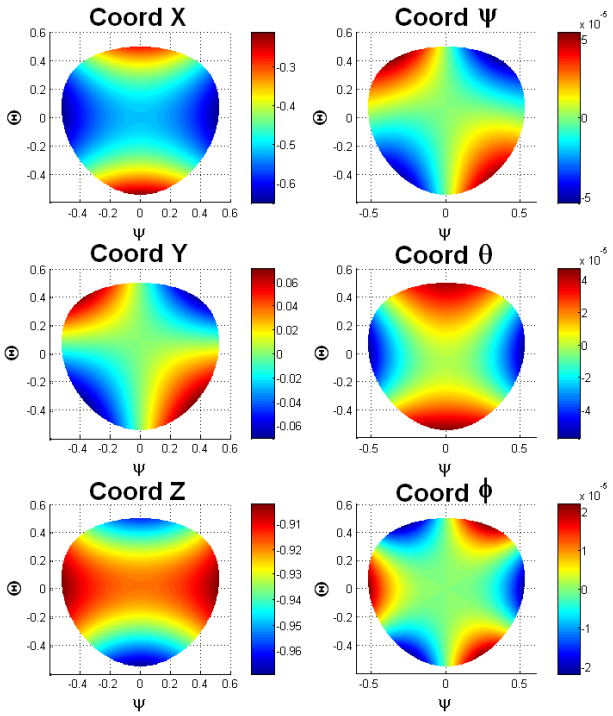

Fig. 7 Error maps due to clearances using a kinetostatic analysis in the workspace with radial clearance at S joints.

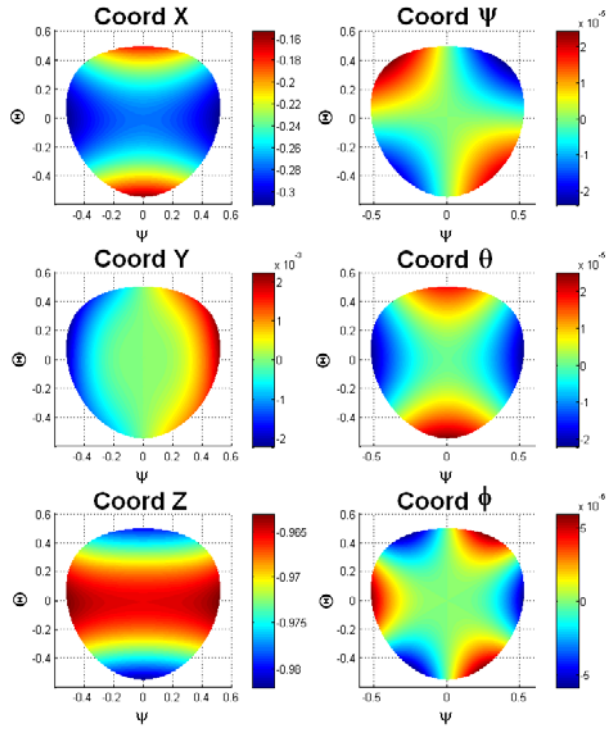

Fig. 8 Error maps due to clearances using a kinetostatic analysis in the workspace with radial clearance at R joints.

Changing the mass distribution of the mobile platform affects to the discontinuities found in the error analysis. Specifically, this section presents the results

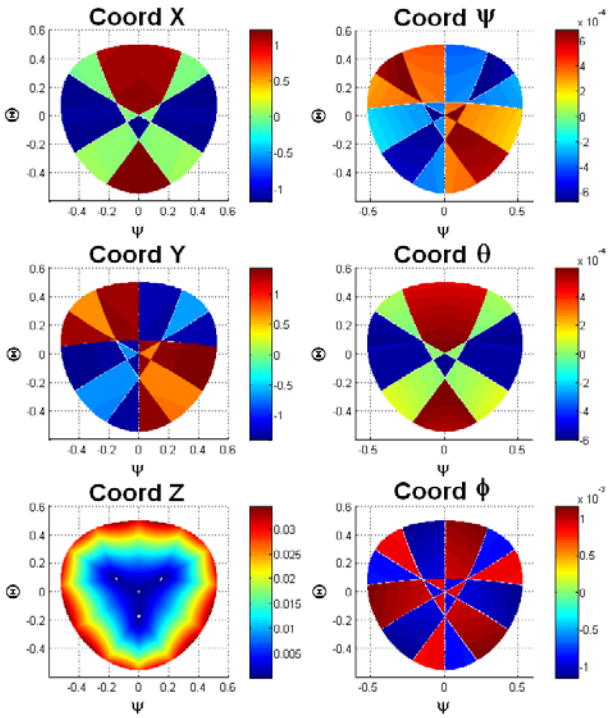

Fig. 9 Error maps due to clearances using a kinetostatic analysis in the workspace with axial clearance at R joints.

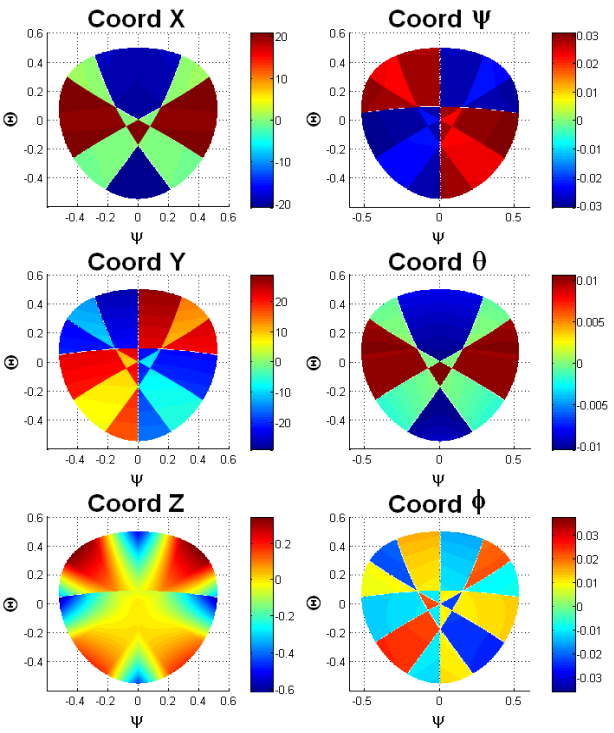

Fig. 10 Error maps due to clearances using a kinetostatic analysis in the workspace with angular clearance at R joints.

of the same mobile platform with a concentrated mass located one metre high over it. If we only suppose radial clearance at revolute joints, error plots result as

shown in Fig. 11.

Error plots of Fig. 11 show discontinuities which did not exist without the added concentrated mass (Fig. 8). Then, the mass added to the mobile platform produces discontinuities in the actual position of the mobile platform. This fact is explained taking into account that the added mass has modified the centre of mass (CM) of mobile platform. This undesired effect can be corrected by adding another mass of the same weight at a symmetric position with respect to the initial CM of the mobile platform. This way, this second mass plays the role of a counterweight and the CM returns to its original position leading to a new error plot without discontinuities, as shown in Fig. 12.

Designers may use a tool like this in order to find discontinuity-free zones where vibrations produced by clearance joint impacts are avoided. Moreover, by modifying the distribution of mass it is possible to create areas free of problems.

4. Dynamic Discontinuity Analysis

However, dynamics can affect dramatically the position of such discontinuity curves. In this section, kinetostatic and dynamics results are compared in order to know how inertial loads affect discontinuities. The trajectory used is an angular motion of the mobile platform about *y* axis with a period T of 5 seconds. Angle Ψ is set to zero and Z coordinate is fixed at 2.05 m, whereas Θ describes a harmonic motion with an amplitude of 0.5 rad. Position, velocity and acceleration of Θ is presented in Fig. 13, whereas parasitic motions [12] and its velocities and accelerations are shown in Fig. 14.

From Fig. 14, it can be observed that parasitic motions period is the half of the period of Θ. Regarding to the magnitude, the one of X coordinate is the highest, while Y and Φ are infinitesimal.

For the described trajectory the changes in the error due to clearances can be observed in Fig. 15, where the black lines correspond to the kinetostatics while the blue ones are calculated taking into account inertial

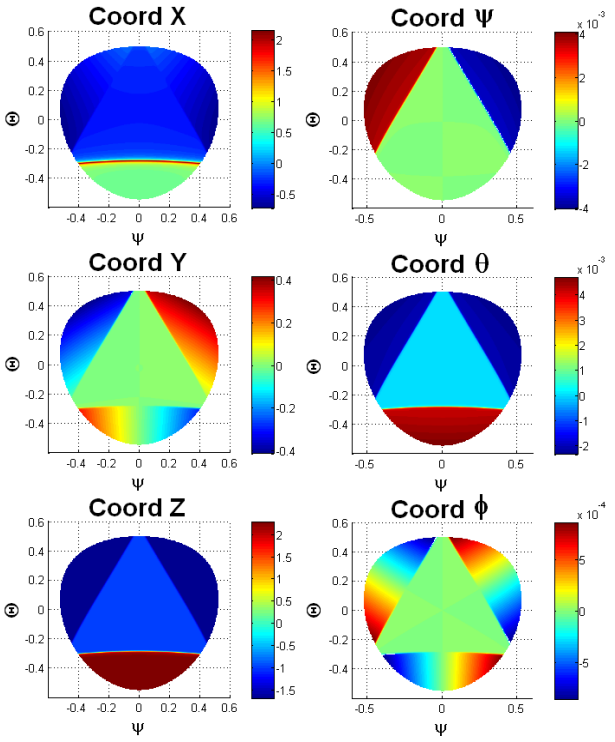

Fig. 11 Error maps due to clearances using a kinetostatic analysis in the workspace with radial clearance at R joints and an additional mass.

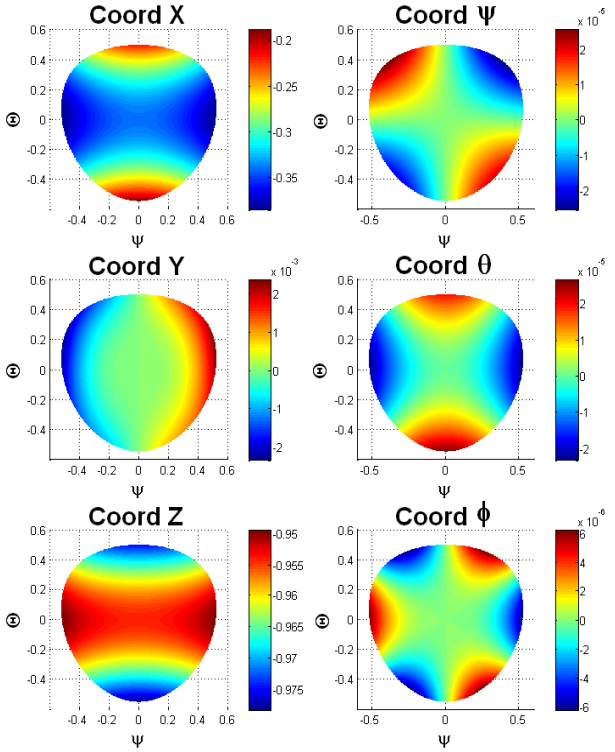

Fig. 12 Error maps due to clearances using a kinetostatic analysis in the workspace with radial clearance at R joints and additional mass and its counterweight.

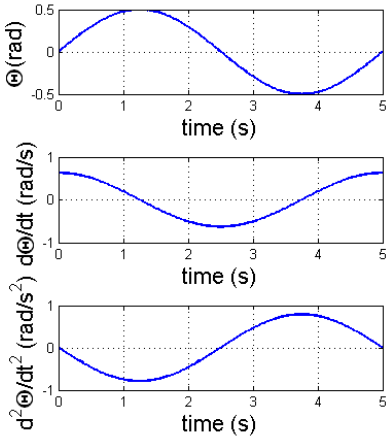

Fig. 13 Position, velocity and acceleration of Θ along the trajectory.

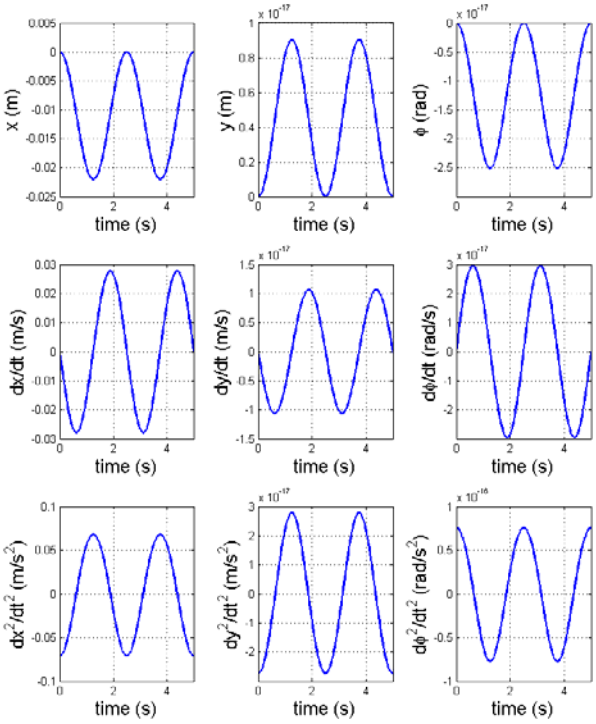

Fig. 14 Parasitic motions along the trajectory.

loads. Θ values are represented on abscissa axis instead of the time and then error results are plotted from 0.25T to 0.75T to avoid repeated values of Θ. The mobile platform has been considered without the additional mass.

Fig. 15 can be analysed together with Fig. 8. Specifically, kinetostatic errors shown in Fig. 15 correspond to those shown by the colour of a vertical line with Ψ equal to zero in Fig 8. For example, in coordinate X, said vertical line of Fig. 8 starts with red

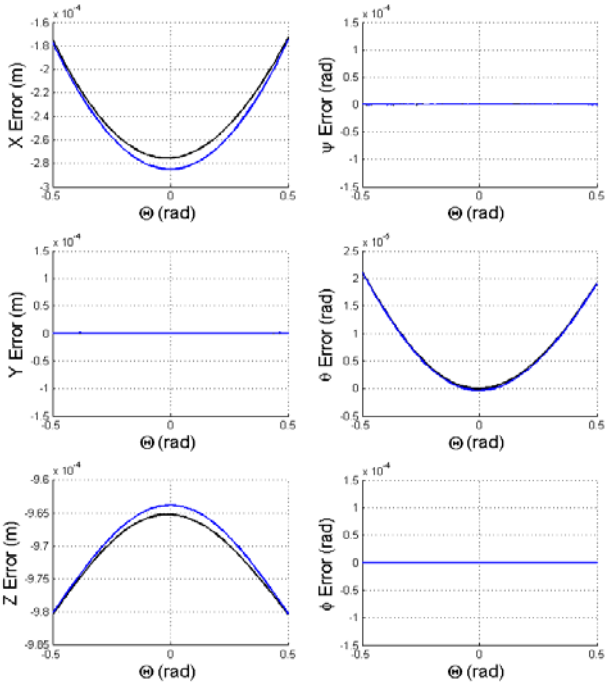

Fig. 15 Position error comparison between dynamics and kinetostatics for Ψ null.

colour for Θ equal to −0.5, when going to higher values of Θ it decreases to blue and then increases again to red when Θ is equal to 0.5. The same values of error can be observed in the black curve of the X coordinate of Fig. 15.

Regarding to the comparison between static and dynamic approaches, Fig. 15 shows that both black and blue lines describe similar error values. In both cases error at coordinate Y and angles Ψ and Φ are almost null, which correspond to green coloured vertical lines shown by Fig. 8. Error at coordinates X and Z have a little difference between black and blue curves and finally error at angle Θ shows almost superimposed black and blue curves. Notice also that these curves can be appreciated in Fig. 8.

If an additional mass is joined to the mobile platform as in section 3, error along the trajectory has substantial changes as was the case of the analysis of the workspace. Fig. 16 shows the position error at *P* along the analysed trajectory.

Black curves of Fig. 16 correspond to vertical lines with Ψ equal to zero of Fig. 11. As far as discontinuities are concerned, sudden changes in colour of the latter

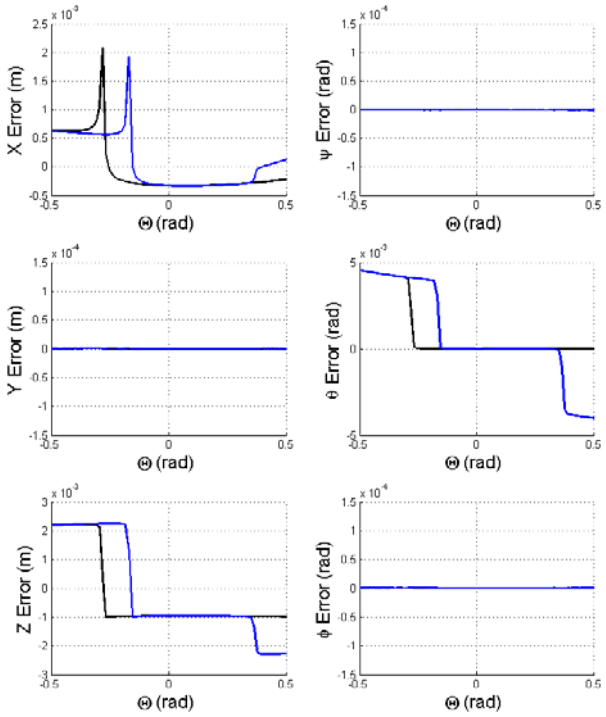

Fig. 16 Position error comparison between dynamics and kinetostatics for Ψ null with an additional mass.

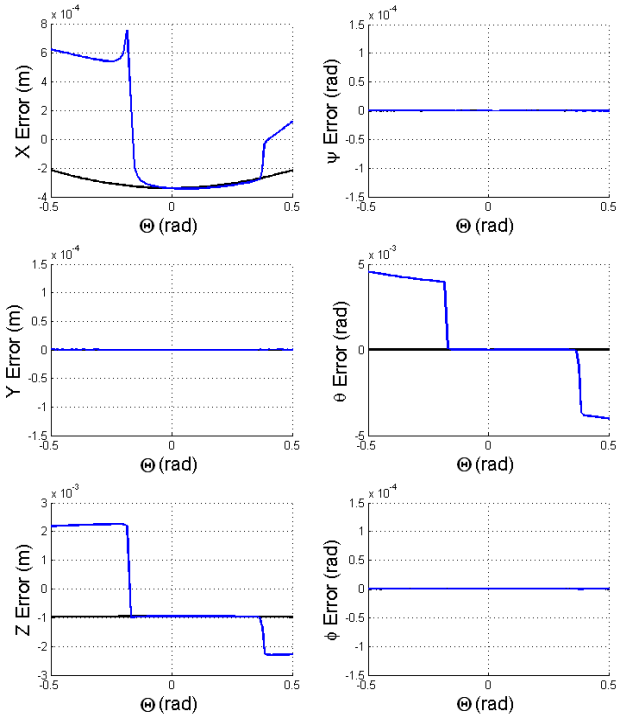

Fig. 17 Position error comparison between dynamics and kinetostatics for Ψ null with an additional mass and its counterweight.

correspond to steps in the black function of the former. On the other hand, inertial loads move the location of the discontinuity from Θ equal to −0.28 to −0.15 rad and they produce another discontinuity when Θ is equal to 0.3 rad.

If another concentrated mass with the role of a counterweight is added as we made in section 3, position error plot results as in Fig. 17.

Now discontinuities disappear in the kinetostatic analysis as was the case of section 3, but they remain (not exactly at the same location) if inertial loads are included. Consequently, returning the CM of the mobile platform to its original position can be effective if inertial loads are negligible. It is not enough when inertial effects play an important role.

5. Conclusions

A numerical procedure for accuracy analysis of parallel manipulators has been presented. Pose error of the end-effector due to clearance is calculated by means of an approximation of the velocity analysis, while the relative position of the two parts of the imperfect joints are determined by means of a kinetostatic or a dynamic analysis.

Analysis of results shows step-like changes on the pose error at certain configurations of the mechanism. These step-like changes lead to discontinuity or uncertainty on the end-effector's actual pose. Mass redistribution can modify such discontinuities.

A comparison between both kinematic and dynamic analysis shows the influence of inertial loads on the pose error.

References

[1] K.-L. Ting, J. Zhu, D. Watkins, The effects of joint clearances on position and orientation deviation of linkages and manipulators, Mechanism and Machine Theory 35 (3) (2000) 391-401.

[2] K.-L. Ting, J. Zhu, Uncertainty analysis of planar and spatial robots with joint clearances, Mechanism and Machine Theory 35 (9) (2000) 1239-1256.

[3] C.R. Tischer, A.E. Samuel, Prediction of the slop in general spatial linkages, International Journal of Robotics Research 18 (8) (1999) 845-858.

[4] J. Meng, D. Zhang, Z. Li, Accuracy analysis of parallel

manipulators with joint clearance, Journal of Mechanical Design 131 (1) (2009) 011013.

[5] S. Venanzi, V. Parenti-Castelli, A new technique for clearance influence analysis in spatial mechanisms, Journal of Mechanical Design 127 (3) (2005) 446-455.

[6] Tsai M-J., Lai T-H. Kinematic sensitivity analysis of linkage with joint clearance based on transmission quality, Mechanism and Machine Theory 39 (11) (2004) 1189-1206.

[7] A.-H. Chebbi, Z. Affi, L. Romdhane, Prediction of the pose errors produced by joints clearance for a 3-UPU parallel robot, Mechanism and Machine Theory 44 (9) (2009) 1768-1783.

[8] O. Altuzarra, J. Aginaga, A. Hernández, I. Zabalza, Workspace analysis of positioning discontinuities due to clearances in parallel manipulators, Mechanism and Machine Theory 46 (5) (2011) 577-592.

[9] P. Flores, J. Ambrósio, Revolute Joints with clerance in multibody systems, Computers and Structures 82 (17-19) (2004) 1359-1369.

[10] P. Flores, J. Ambrósio, J.C.P. Claro, H.M. Lankarani, C.S. Koshy, A study on dynamics of mechanical systems including joints with clearance and lubrication, Mechanism and Machine Theory 41 (3) (2006) 247-261.

[11] I. Khemili, L. Romdhane, Dynamic analysis of a flexible slider-crank mechanism with clearance, European Journal of Mechanics A/Solids 27 (5) (2008) 882-898.

[12] J.A. Carretero, R.P. Podhorodeski, M.A. Nahon, C.M. Gosselin, Kinematic analysis and optimization of a new three degree-of- freedom spatial parallel manipulator, Journal of Mechanical Design 122 (1) (2000) 17-24.

[13] J.-P. Merlet, Parallel Robots, Springer, 2006.

[14] V. Parenti-Castelli, S. Venanzi, On the joint clearance effects in serial and parallel manipulators, in: Proceedings of the Workshop on Fundamental Issues and Future Research Directions for Parallel Mechanisms and Manipulators, Quebec, Canada, October 3-4, 2002, pp. 215-223.